Particle-hole excitations in small metal clusters by electron scattering

M. R. Spinella, M. Bernath, and O. Dragún
Departamento de Física, Comisión Nacional de Energía Atómica, Avenida del Libertador 8250, 1429 Buenos Aires, Argentina

H. Massmann
Departamento de Física, Facultad de Ciencias, Universidad de Chile, Casilla 653, Santiago de Chile, Chile
(Received 2 January 1996)

A theoretical evaluation of inelastic transition amplitudes corresponding to collisions between low-energy electrons (up to 5 eV) and small metallic clusters is presented. The target is excited into a particle-hole state and the cross section is obtained in the Born approximation. The formalism is applied to the Na_8 cluster. Form factors for the direct and exchange-correlation terms of the residual interaction are shown as well as angle-integrated cross sections as a function of the energy of the incident electron. These cross sections present resonances associated with quasibound states in the outgoing and/or incoming channels at incident energies related to the Na_8 single-particle states through the Q values of the transitions. The results also show the importance of the inclusion of the residual exchange-correlation contribution. [S1050-2947(96)06408-6]

PACS number(s): 36.40.−c, 34.80.−i,

I. INTRODUCTION

The simple shell structure description for the valence electrons in metal clusters has proved to be a very useful model for the interpretation of a wide variety of experiments [1,2]. Indeed, cluster stabilities, relative abundances, and ionization potentials are some of the physical magnitudes that have been predicted and reproduced with a reasonable level of accuracy by theories based on the shell-model description.

Other kinds of experiments are those in which photons are absorbed by clusters. These experiments, which allow the study and analysis of atomic polarizabilities and plasmon resonances [3], have shown the necessity of a theory that goes beyond the main field assumption. These more refined calculations take into account the residual interaction between the valence electrons and thereby are able to explain the intrinsic structure of the plasmon excitations in terms of the collective motion of the electrons [4].

The scattering of low-energy electrons also can be used to explore the cluster structure. We are particularly interested in the knowledge that can be obtained from this kind of experiment, although the data so far are very scarce.

Recently some cluster beam depletion experiments produced by low-energy electrons impinging on Na_8, Na_{20}, and Na_{40} clusters have been published [5]. These experiments allowed the measurement of integrated inelastic cross sections for processes in which the clusters suffer electron attachment and/or fragmentation.

More information could be extracted from electron-scattering experiments if experimental techniques were able to resolve the energy and angular distributions of the outgoing electrons. In particular, for very slow incoming electrons, where processes such as cluster fragmentation are negligible, the incident electron will interact with the cluster, leaving it in an excited residual state. When the incident electron promotes a bound valence electron from a state under the Fermi level to a state above the Fermi level, there will be a particle-hole excitation. If, on the other hand, the residual state is characterized by a cloud of valence electrons moving coherently, a collective state will be excited in the cluster, like the plasmon states mentioned above.

At very low energies, the most important process taking place in an electron-cluster collision will always be the elastic scattering. We recently studied the elastic scattering of low-energy electrons by neutral [6] and ionized [7] sodium clusters and found that the total integrated cross section exhibits strong resonances as a function of the incident electron energy. These resonances can be correlated to the existence of quasibound states in the electron-target system and turn out to be sensitive to the particular choice of the electron-cluster interaction. We conclude that an experimental study of elastic electron scattering by clusters will be useful to gain insight into the details and contributions of the mean-field potential.

In this paper we go a step further and present a theoretical analysis of inelastic collisions between electrons and metal clusters by considering the simplest excitation, which is of single-particle-hole character, within the framework of a Born approximation. There are other excitations such as collective states (expected for energies above 3 eV for the Na_8 cluster) and core excitations (probably very weak) that will also contribute to the total inelastic cross section. Such contributions, which do not affect the results for very low incoming electron energies, once evaluated, will have to be added incoherently to the inelastic cross section studied in the present work. There is a complete lack of experimental results in that direction so far, but it is our aim to stimulate research toward this kind of experiment, in view of the interesting information it may provide.

In Sec. II we present a formalism that leads to the scattering amplitudes and cross section. In Sec. III the scattering wave functions are obtained for the Na_8 cluster, the only case to which the formalism will be applied in this work. Another important ingredient, defined in Sec. II, are the radial form factors for single-particle excitations; these are analyzed in Sec. IV. In Sec. V the different elements are

combined and inelastic cross sections are evaluated. The conclusions are presented in Sec. VI.

II. FORMALISM

As is often done when studying metal clusters, during the development of the formalism we will refer to ideas from the field of nuclear physics, in particular to the nuclear reaction theory. The study of electrons (and also nucleons) colliding with nuclear targets has been a powerful tool to learn about the nuclear structure, charge distribution in nuclei, mean-field potential, single-particle energies, excited states in nuclei, and many other properties. We expect that the study of analogous collisions in the metal cluster field will also yield useful knowledge.

We start with the premise that at sufficiently low energies the elastic scattering is the most important process to occur when electrons collide with a metal cluster. We furthermore assume that at these low energies the inelastic excitation that does appear occurs as a one-step process. In that case the inelastic transition amplitude, in the Born approximation, can be written as

$$T_{1\to 2}=\int \chi^f(\vec{k}_f,\vec{R})\langle\phi_2(\vec{r})|V_{\rm res}(\vec{r},\vec{R})|\phi_1(\vec{r})\rangle\chi^i(\vec{k}_i,\vec{R})d\vec{R}. \tag{2.1}$$

Let us describe the various components of this expression. The wave functions χ describe the motion of the incoming electron in the field generated by the target cluster, $\vec{k}_i$ and $\vec{k}_f$ being the wave vectors in the initial and final channels. These wave vectors define the orientation of the incoming and outgoing electrons. In Sec. III we will propose a mean-field interaction for the electron-target system and discuss the characteristics of the wave functions for the initial and final channels. The formalism takes into account the Q effect, that is, the kinetic-energy difference in both channels due to the transfer of energy from the incident electron to the target cluster. The coordinate $\vec{R}$ describes the position of the incoming electron, while $\vec{r}$ gives the position of the valence electron, both with respect to the center of the cluster. The internal wave functions for the valence electrons

$$\phi_i(\vec{r})=\frac{u_{n_il_i}(r)}{r}Y_{l_im_i}(\theta,\phi)\quad (i=1,2) \tag{2.2}$$

are obtained in a shell-model approach for the clusters (see Sec. IV). The residual potential $V_{\rm res}$ is the interaction responsible for the particle-hole excitation, while the relative wave function in the ingoing channel can be written in a partial-wave expansion as

$$\chi^i(\vec{k}_i,\vec{R})=\frac{4\pi}{k_iR}\sum_{l=0}^{\infty} i^l f_l(k_i,R)\sum_{m=-l}^{l} Y_{lm}(\hat{R})Y^*_{lm}(\hat{k}_i)$$
$$=\frac{\sqrt{4\pi}}{k_iR}\sum_{l=0}^{\infty}\hat{l}i^l f_l(k_i,R)Y_{l0}(\Theta,0), \tag{2.3}$$

where $\cos(\Theta)=\hat{R}\cdot\hat{k}_i$. In a similar way, for the outgoing wave function one obtains

$$\chi^f(\vec{k}_f,\vec{R})=\frac{4\pi}{k_fR}\sum_{l'=0}^{\infty}\sum_{m'=-l'}^{l'} i^{l'}\tilde{f}_{l'}(k_f,R)Y_{l'm'}(\Theta,\Phi)Y^*_{l'm'}(\hat{R}). \tag{2.4}$$

In the previous relations, $f_l(k_i,R)$ and $\tilde{f}_{l'}(k_f,R)$ are the partial radial wave functions of angular momentum l and l', respectively, and (Θ,Φ) are the angle coordinates of the outgoing electron.

The incoming electron-cluster residual interaction has a direct and an exchange-correlation contribution given, in the scope of the approximations we are using for the mean field, by [4]

$$V_{\rm res}(\vec{R}-\vec{r})=\frac{e^2}{|\vec{R}-\vec{r}|}+\frac{dV_{\rm xc}(\rho)}{d\rho}\delta(\vec{R}-\vec{r}). \tag{2.5}$$

Here

$$V_{\rm xc}(\rho)=\frac{d\epsilon_{\rm xc}(\rho)}{d\rho} \tag{2.6}$$

is the exchange-correlation potential of Gunnarsson and Lundqvist [8], $\epsilon_{\rm xc}(\rho)$ is the exchange-correlation energy density, and ρ is the radial density of the valence electrons of the cluster

$$\rho(r)=\frac{1}{4\pi}\sum_i\left|\frac{u_{n_il_i}(r)}{r}\right|^2. \tag{2.7}$$

Expanding the direct term of Eq. (2.5)

$$\frac{e^2}{|\vec{R}-\vec{r}|}=\sum_{\lambda,\mu}\frac{4\pi e^2}{\hat{\lambda}^2}\frac{r_<^\lambda}{r_>^{\lambda+1}}Y^*_{\lambda\mu}(\theta,\phi)Y_{\lambda\mu}(\hat{R}), \tag{2.8}$$

after some algebra, the direct contribution T_d to the $1\to 2$ particle-hole transition is obtained. Using atomic units, for a given m_1 and m_2, this is given by

$$T_d(\Theta,\Phi)=\frac{(4\pi)^{3/2}}{k_fk_i}\sum_{ll'\lambda}\hat{l}^2\hat{l}'\hat{l}_1\hat{l}_2(-1)^{m_2}\begin{pmatrix}\lambda & l_1 & l_2\\ 0 & 0 & 0\end{pmatrix}$$
$$\times\begin{pmatrix}\lambda & l_1 & l_2\\ \mu & m_1 & -m_2\end{pmatrix}\begin{pmatrix}l & \lambda & l'\\ 0 & 0 & 0\end{pmatrix}$$
$$\times\begin{pmatrix}l & \lambda & l'\\ 0 & \mu & -\mu\end{pmatrix}Y_{l'-\mu}(\Theta,\Phi)$$
$$\times\int_0^\infty dR f_l(k_i,R)R^\lambda_{12}(R)\tilde{f}_{l'}(k_f,R). \tag{2.9}$$

The direct radial form factor

$$[R^\lambda_{12}(R)]_d=\int dr u_{n_2l_2}(r)\frac{r_<^\lambda}{r_>^{\lambda+1}}u_{n_1l_1}(r) \tag{2.10}$$

(as well as the exchange correlation radial form factor; see below) has the structure information about the $1\rightarrow 2$ transition of the cluster.

For the evaluation of the exchange-correlation amplitude $T_{\rm xc}$, we use the exchange-correlation energy density expression of Gunnarsson and Lundqvist [8], which leads to the $V_{\rm xc}$ potential

$$V_{\rm xc}=-\frac{1.222}{r_s(r)}-0.0666\ \ln\left(1+\frac{11.4}{r_s(r)}\right), \tag{2.11}$$

where $r_s(r)=[3/4\rho(r)]^{1/3}$ is the local value of the Wigner-Seitz radius. Then

$$\frac{\partial V_{\rm xc}}{\partial\rho}=-\frac{2}{3}\left(\frac{3}{2\pi}\right)^{2/3}\frac{1}{\rho(r)r_s(\rho(r))}-\frac{0.0222}{1+\dfrac{r_s(\rho(r))}{11.4}\rho(r)}. \tag{2.12}$$

Expanding the δ function of Eq. (2.5) in angular momentum components, an expression similar to Eq. (2.9) is obtained for the exchange-correlation amplitude $T_{\rm xc}$, but with a form factor given by

$$[R^{\lambda}_{12}(R)]_{\rm xc}=\frac{2\lambda+1}{4\pi}u_{n_1l_1}(R)\frac{\partial V_{\rm xc}}{\partial P(R)}u_{n_2l_2}(R). \tag{2.13}$$

The coherent sum of T_d and $T_{\rm xc}$ gives the total transition amplitude corresponding to the excitation of a valence electron from the state (n_1,l_1,m_1) to the state (n_2,l_2,m_2) with an electron emerging with energy $E_f=k_f^2/2$. After summing over all possible orientations and averaging over the initial projections we get the differential cross section for the excitation

$$\frac{d\sigma_{i\rightarrow f}(\Theta)}{d\Omega}=\frac{1}{4\pi^2}\frac{k_f}{k_i}\frac{1}{2l_1+1}\sum_{m_1,m_2}|T_d+T_{\rm xc}|^2. \tag{2.14}$$

III. INCOMING AND OUTGOING WAVE FUNCTIONS

To obtain the wave functions for the incoming and outgoing channels, we must solve the radial Schrödinger equation for the partial components $f_l(k,r)$,

$$\left[\frac{d^2}{dr^2}-\frac{l(l+1)}{r^2}-\frac{2m}{\hbar^2}V_{\rm opt}+k^2\right]f_l(k,r)=0. \tag{3.1}$$

A crucial point is the choice of the average optical potential $V_{\rm opt}$ between the electron projectile and the cluster target. This problem was exhaustively discussed in a previous paper [6]. As a first approximation $V_{\rm opt}$ can be assumed to be the local-density approximation (LDA) mean-field potential plus a term arising from the polarization of the valence cloud due to the incoming electron. Thus

$$V_{\rm opt}=V_{\rm LDA}+V_{\rm pol}, \tag{3.2}$$

where $V_{\rm LDA}$ was obtained by solving the Kohn-Sham equations within the jellium model and has the typical jellium, Coulomb, and exchange-correlation contributions, the latter evaluated within the Gunnarsson-Lundqvist approach. For low bombarding energies the local adiabatic approximation for the polarization term may be used [9,10]

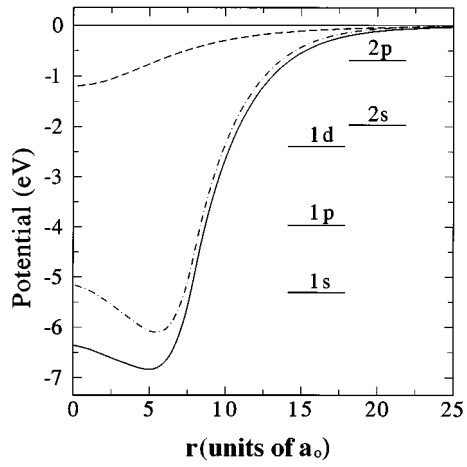

FIG. 1. Mean-field potentials for Na_8 in the local-density approximation (LDA) to density-functional theory. The dashed line shows the polarization contribution, the dot-dashed line corresponds only to the LDA contribution, while the solid line displays the total potential (LDA plus polarization). Distances are expressed in a_0 the Bohr radius. On the right-hand side of the figure, the energies of the single-particle bound states are shown for the total potential (polarization included).

$$V_{\rm pol}(r)=\frac{-\alpha e^2}{2(d^2+r^2)^2}, \tag{3.3}$$

where α is the cluster polarizability and d is a cutoff parameter of the order of the cluster size [9,10]. In [6] it was shown that variations of d of about 15% affect only the fine details of the cross section. The static polarizability α was obtained from experiment [3]. Within this frame, and neglecting possible absorption effects, i.e., imaginary contributions to the optical potential (see Ref. [6] for a discussion of this point), the wave functions for a given incident energy can be evaluated.

Figure 1 shows the resulting optical potential for the e-Na_8 system. In order to appreciate the importance of the polarization we display in Fig. 1 also the potential without the polarization correction.

The asymptotic behavior of the radial wave functions $f_l(r)$ is

$$f_l(k,r)\rightarrow\frac{1}{2i}[e^{-i(kr-l\pi/2)}-e^{2i\delta_l}e^{i(kr-l\pi/2)}], \tag{3.4}$$

where $e^{2i\delta_l}=S_l$ is the scattering matrix and δ_l is the phase shift. In Fig. 2 we show the phase shifts for the elastic channel of the e-Na_8 system for different angular momenta as a function of the incident energy. The rapid increase of the phase shifts at given energies indicates the presence of resonances. These resonances can be related to the existence of quasibound states with a definite angular momentum [6]. Only l values less than 15 were considered in the calculations since higher-l values do not contribute to the phase shifts for energies less than 5 eV.

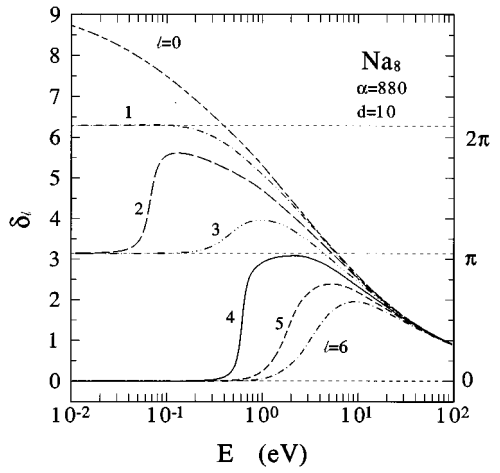

FIG. 2. Phase shifts from $l=0$ up to $l=6$ as a function of the incident electron energy for the e^--Na_8 system using the total potential of Fig. 1.

IV. THE FORM FACTOR

To evaluate the radial form factors we must first determine the intrinsic bound wave functions $\phi_i(\vec{r})=u_{n_i l_i}(r)/r$, $i=1,2$. These wave functions were obtained by diagonalizing the self-consistent potential arising from the Kohn-Sham equations in the local-density approximation plus the polarization contribution. The single-particle energies for all the bound states of the system, for the total LDA plus polarization potential, are also shown in Fig. 1.

It can be argued than a better single-particle wave function is obtained by taking into account self-interaction corrections (SICs) [11] in the Kohn-Sham equations, which introduce state-dependent potentials to the formalism. This, however, for the present calculations, is only a minor correction, as can be observed from the following. In Fig. 3 the five bound wave functions $u_{n,l}$, obtained within the LDA, are shown. Also displayed are the wave functions resulting by introducing SICs in the calculation. Figure 3(a) shows the wave functions for the initially occupied states. For the other bound states, there exist two sets of SIC wave functions, one set coming from the diagonalization of the $1s$ potential [Fig. 3(b)] and the other for the case that the initial state of the valence electron is $1p$ [Fig. 3(c)]. As can be seen from the figures, the SIC and LDA wave functions do not differ significantly and therefore in the following we will use the simpler LDA set.

As discussed in Sec. II, the residual interaction consists of a direct and an exchange-correlation term, each leading to a corresponding contribution to the form factor. As can be seen from expressions (2.9), (2.10), and (2.13), the formalism also separates the contributions coming from the different multipolarities of the residual potential. In the following we will consider the allowed particle-hole transitions $1\rightarrow 2$ of the Na_8 cluster: $1s\rightarrow 1d$, $1s\rightarrow 2p$, $1s\rightarrow 2s$, $1p\rightarrow 1d$, $1p\rightarrow 2s$, and $1p\rightarrow 2p$ (see also Fig. 1). From the Clebsch-Gordan coefficients in Eq. (2.9) we deduce that all transitions occur for a single multipolarity λ, except the fourth of these, for which $\lambda=1,3$, and the sixth, for which $\lambda=0,2$. We therefore have eight form factors $R^{\lambda}_{1\rightarrow 2}(R)$, which are shown in Fig. 4. Figure 4(a) displays the form factors associated with the direct part of the residual interaction. The transitions $1s\rightarrow 2s$ and $1p\rightarrow 2p$ with $\lambda=0$ are dominant near the origin and for these cases the excitation has a larger probability of taking place inside the cluster.

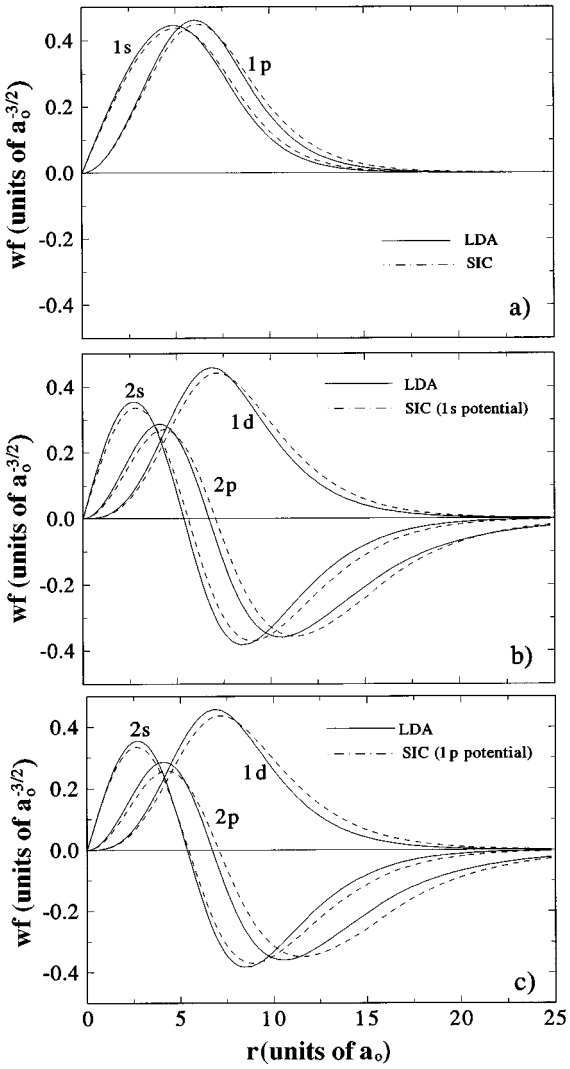

FIG. 3. Electron valence bound wave functions obtained in two different approaches. For the two occupied states of Na_8 we show (a) the result of the LDA calculation compared with a calculation including self-interaction corrections (SICs). The LDA results are compared with the SIC wave functions of (b) the $1s$ potential and (c) the $1p$ potential. As can be seen, results are very similar for both approaches.

Figure 4(b) corresponds to the total (direct plus exchange correlation) form factors. The inclusion of the exchange-correlation generally reduces the magnitude of the form factors and shifts the curves towards larger distances.

The form factor for the $1p\rightarrow 2p$ transition, with $\lambda=2$, which has its maximum at around $R=26$ a.u., seems to be the dominant term. However, once the integration with the oscillating ingoing and outgoing wave functions is performed, its contribution to the final inelastic cross section turns out to be negligible. Even though it is not shown in Fig. 4, for very large distances all the form factors converge to zero.

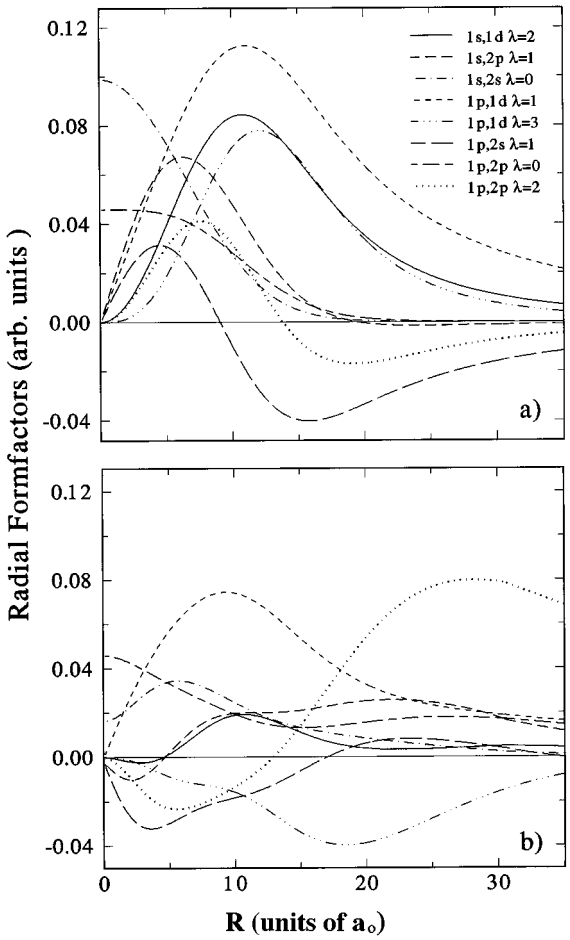

FIG. 4. Radial form factors for the (a) direct and (b) direct plus exchange-correlation contributions to the residual interaction. We display the form factors corresponding to all the possible transitions and we also detail the angular momentum of the multipolar expansion in Eq. (2.9).

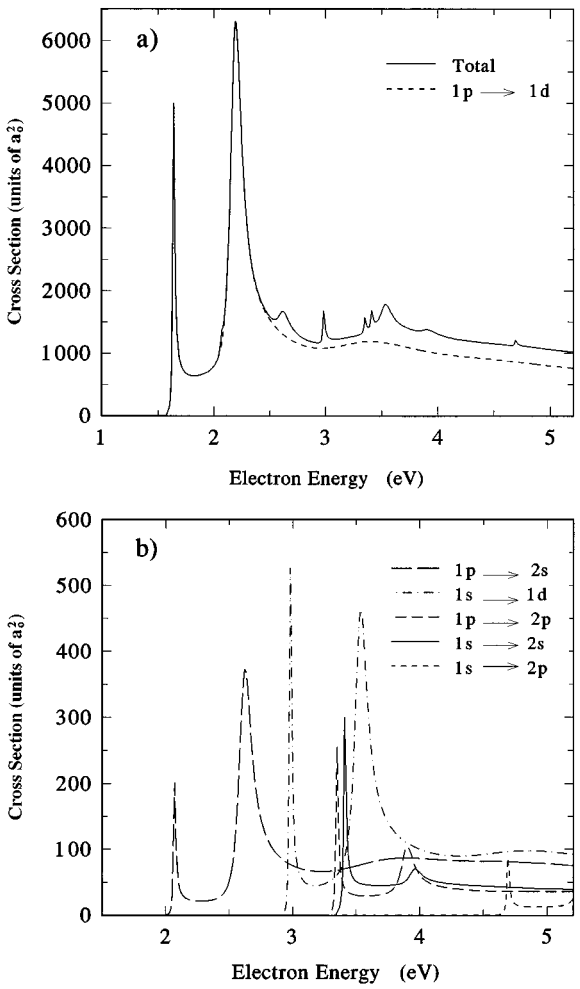

FIG. 5. (a) Direct angle-integrated cross sections for the system e-Na_8 as a function of the energy of the incident electron. The different contributions of the particle-hole transitions are added incoherently to obtain the total cross section (full line). The dashed line shows the individual contribution of the dominant $1p \rightarrow 1d$ transition. (b) Direct angle-integrated cross sections for each of the other (different of $1p \rightarrow 1d$) particle-hole transitions. The scale is magnified with respect to (a) to appreciate how channels open progressively when the incoming energy increases. Each transition shows two resonances: the first at an energy of $Q+0.08$ eV and the second one at $Q+0.62$ eV.

V. THE TOTAL CROSS SECTION

In Fig. 5(a) we show the total angle-integrated cross section for the collision e-Na_8 as a function of the energy of the incoming electron, using only the direct residual interaction (i.e., without considering the exchange-correlation part). The contribution of the $1p \rightarrow 1d$ transition, which almost exhausts the total cross section for the considered incoming energy range, is also shown. The small differences between the two curves in Fig. 5(a) come from the contribution of all the other single-particle-hole transitions, which are plotted in detail in Fig. 5(b) (note the changes in the scale between the two figures).

The opening of each inelastic channel occurs when the incoming energy coincides with the Q value of the corresponding particle-hole transition. These Q values (or threshold energies) are summarized in Table I. It is interesting to remark that these values depend on the details of the mean field used in the calculation.

Another general feature of each transition contribution is that they present two maxima (resonances) at approximately 0.08 and 0.62 eV above their threshold enery. These resonances can be explained by analyzing the radial integrals

$$A_{1,2,l,l',\lambda} = \int_0^\infty dR f_l(k_i,R) R_{12}^{\lambda}(R) \tilde{f}_{l'}(k_f,R), \qquad (5.1)$$

which appear in the expression (2.9) for the direct transition amplitude.

In these radial integrals, an overlap is performed between the form factor and ingoing and outgoing relative wave functions. It is well known that the magnitude of the radial wave functions, in the interior of the cluster, increases significantly when the bombarding energy coincides with (or is close to) a quasistationary resonant state [6]. Two of these resonances can clearly be identified from the phase shifts shown in Fig. 2: one for $l=2$ at 0.08 eV and another for $l=4$ at 0.62 eV. These two energies plus the transitions thresholds energies constitute the incoming energies at which the peaks in Figs. 5(a) and 5(b) are observed (see also Table I).

TABLE I. Summary of the relevant magnitudes corresponding to the resonances of the integrated cross sections. An asterisk denotes a weak contribution.

Transition	Q (eV)	Inelastic resonance (eV)	Outgoing electron energy (eV)	Dominant incoming l	Dominant outgoing l'	Multipolarity λ
$1p\rightarrow 1d$	1.57	1.65	0.08	3*	2	1
				5	2	3
		2.19	0.62	5	4	1
				6*	3*	3*
$1p\rightarrow 2s$	2.00	2.08	0.08		2	1
		2.62	0.62	5*	4	1
$1s\rightarrow 1d$	2.91	2.99	0.08	4*	2	2
		3.53	0.62	6	4	2
$1p\rightarrow 2p$	3.28	3.36	0.08		2	0–2
		3.90	0.62	6	4	2
$1s\rightarrow 2s$	3.34	3.42	0.08		2	0
		3.96	0.62		4	0
$1s\rightarrow 2p$	4.62	4.70	0.08		2	1

We illustrate the previous discussion analyzing in detail the most important contribution to the inelastic cross section: the $1p\rightarrow 1d$ transition [see Fig. 5(a)]. The resonances of this contribution occur for bombarding energies (which are the energies of the ingoing wave function) in the vicinity of 1.65 and 2.2 eV, respectively (see Table I). For the corresponding outgoing radial wave functions, the energies (after substracting the Q value) are 0.08 and 0.62 eV. This suggests strongly that the two peaks are due to the $l'=2$ and $l'=4$ outgoing radial wave functions, respectively. This is confirmed when the radial integrals $A_{1,2,l,l',\lambda}$ are evaluated. Figure 6 shows these for the second resonance and $\lambda=1$. It is found that the largest term indeed occurs for $l'=4$ (and $l=5$).

Using a similar argument, it is possible to understand the resonances for all particle-hole transitions. In Table I the dominant ingoing l and outgoing l' values, as well as the multipolarity λ, are given for all resonances.

It is also possible to understand why the inelastic $1p\rightarrow 1d$ transition is particularly strong. From the discussion in the previous paragraph it was found that, for the 2.2-eV resonance, the most important ingoing angular momentum of the radial wave function is $l=5$. As can be seen from Fig. 2, a large wave function in the interior of the cluster is expected, due to a wide resonance that occurs at precisely that ingoing energy and l value. The large maximum in the inelastic cross section for the $1p\rightarrow 1d$ transition is therefore due to a $\lambda=1$ well-matched condition with resonances in the ingoing as well as outgoing wave functions.

Another ingredient that contributes to the dominance of the $1p\rightarrow 1d$ transition is its particularly large form factor (see Fig. 4), which arises from the strong overlap of the involved single-particle wave functions.

In Fig. 7(a) we show the total calculation using the LDA potential when also the exchange and correlation parts of the residual interactions are included. The cross section decreases considerably, indicating the importance of the exchange-correlation effects, as is usually found in metal cluster physics. The general features persist and the interpretation given above remains valid for this case. The order of magnitude of the obtained cross section is about 500 bohrs^2, which is of the order of the inelastic cross section obtained in Ref. [5] for other processes such as fragmentation or electron attachment. A comparison of this magnitude with the 4000 bohrs^2 obtained in Ref. [6] (see Fig. 6 of [6]) for the elastic scattering justifies the use of the Born approximation in the present paper. We also show in Fig. 7(b) results of a more complicated calculation using the SIC to the

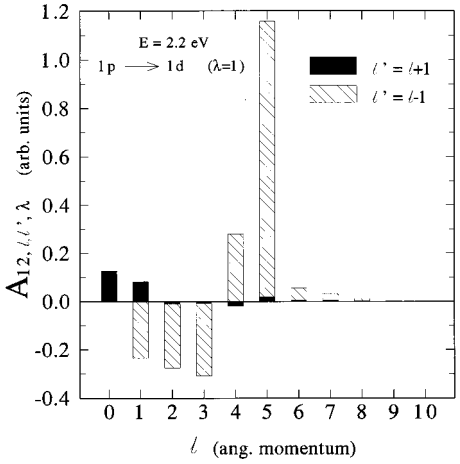

FIG. 6. Relative magnitudes of the $A_{1,2,l,l',\lambda}$ integrals for an incident energy of 2.2 eV and for the outgoing angular momenta $l'=l+1$ and $l'=l-1$. The transition displayed is the $1p\rightarrow 1d$ with $\lambda=1$. As can be seen, the dominant contribution corresponds to $l=5$ and $l'=4$.

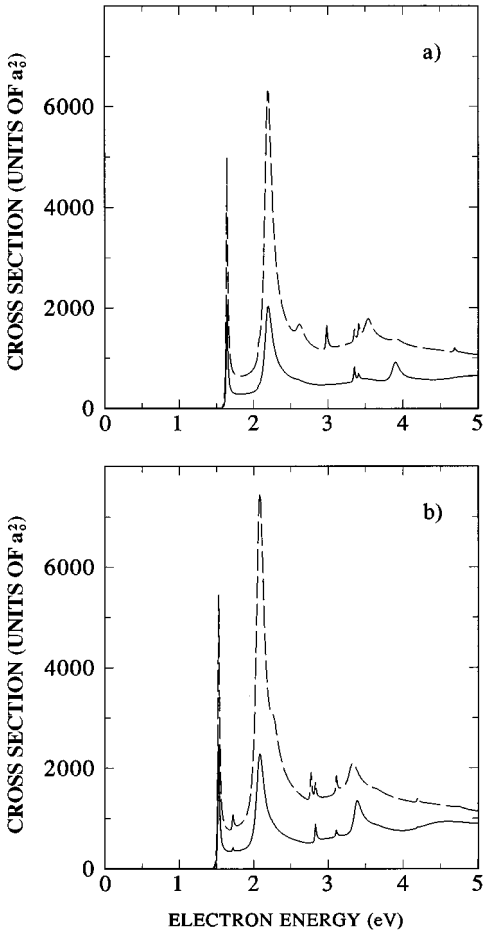

FIG. 7. (a) Comparison between total angle-integrated cross sections. The solid line displays the calculation including direct and exchange correlations terms and the dashed line shows only the direct case. (b) Same as (a), but using the SIC to the LDA potential for the single-particle wave functions.

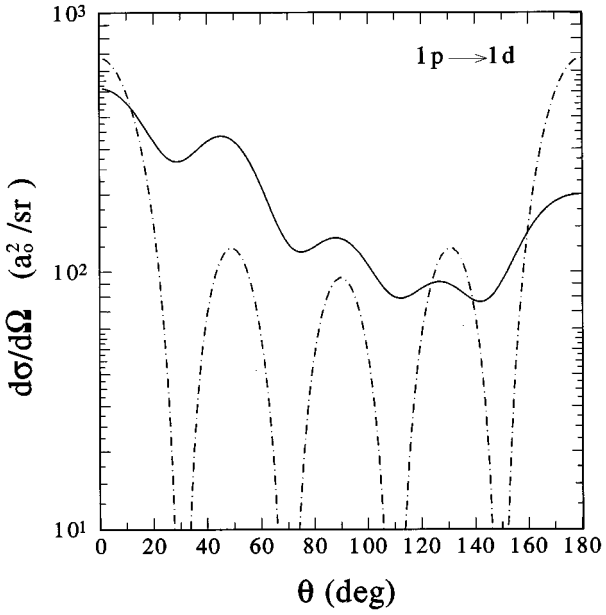

FIG. 8. Differential cross section as a function of the scattering angle for the dominant transition $1p \rightarrow 1d$. The incident energy is 2.2 eV at which a resonance in the total cross section appears. The angular distribution has four minima following the zeros of $P^2_{l=4}$, which is also shown in the figure by a dashed line.

LDA for the wave functions of the single-particle states. Essentially, an overall energy shift of about -0.25 eV is observed. This shift is a consequence of the differences between the single-particle energies obtained in each approximation.

Finally, we show in Fig. 8 a differential cross section corresponding to the incident energy $E=2.2$ eV. The calculation performed includes the direct and exchange-correlation contributions. The results reflect the influence of the partial waves mentioned above. At this incoming energy the angular distribution oscillates in a pattern reminiscent of $P_{l'=4}$, which has been shown to dominate the $1p \rightarrow 1d$ transition. This indicates that an experimental angular distribution, if performed, could yield valuable information. Summarizing, the interesting feature of the present analysis is that inelastic electron scattering could provide an experimental tool to learn about the single-particle transition energies and to explore the shell structure of metal clusters.

VI. CONCLUSION

In this paper we present an approach to the calculation of inelastic cross sections in low-energy electron-cluster collisions when the excited state of the cluster is of particle-hole type. We show that very interesting information can be extracted concerning the structure of the cluster and in this sense the experiment would be an indirect measurement of the energies of the particle-hole transitions and, as a consequence, a test for the validity of a given mean field.

We show that the total cross section has maxima associated with resonances in the elastic channels, also reflected in the angular distributions. The dominant resonances of the $1p \rightarrow 1d$ transition can be explained in terms of a well-matched inelastic transition in which resonances occur in both the incoming and outgoing elastic channels. We also observe that to have a correct description of the inelastic process at these low incoming energies, we must consider in the theory the Q values of the transitions, i.e., the energy difference between the single-particle levels involved in the reaction. The total calculation including the exchange and correlation contribution to the residual potential indicates the relevance of these terms in the total cross section. The experimental results in this field so far are scarce, although we hope to stimulate, through this paper, experimental research on electron-cluster collisions.

ACKNOWLEDGMENTS

We appreciate support from Fundacion Antorchas, Argentina and FONDECyT, Chile under Project No. 1940229. We thank J. M. Pacheco for providing us the SIC potentials and useful discussions. M.R.S. and M.B. also acknowledge support from CONICET, Argentina.

[1] W. A. de Heer, Rev. Mod. Phys. **65**, 611 (1993), and references therein.
[2] M. Brack, Rev. Mod. Phys. **65**, 677 (1993), and references therein.
[3] K. Selby *et al.*, Phys. Rev. B **40**, 5417 (1989); **43**, 4565 (1991).
[4] C. Yannouleas *et al.*, Phys. Rev. Lett. **63**, 255 (1989); C. Yannouleas and R. A. Broglia, Phys. Rev. A **44**, 5793 (1991).
[5] V. V. Kresin, A. Scheidemann, and W. D. Knight, Phys. Rev. A **44**, R4106 (1991).
[6] M. Bernath, O. Dragún, M. R. Spinella, and H. Massmann, Z. Phys. D **33**, 71 (1995).
[7] M. Bernath, O. Dragún, M. R. Spinella, H. Massmann, and J. Pacheco, Phys. Rev. A **52**, 2173 (1995).
[8] O. Gunnarsson and B. I. Lundqvist, Phys. Rev. B **13**, 4274 (1976).
[9] C. Joachain, *Quantum Collision Theory* (North-Holland, Amsterdam, 1983).
[10] M. Mittelman and K. Watson, Phys. Rev. **113**, 198 (1959).
[11] J. M. Pacheco and W. Eckardt, Ann. Phys. (N.Y.) **1**, 254 (1992).